Available Transfer Capability Determination using Bifurcation Criteria and its Enhancement through SVC Placement

Sanjay K. Chaudhary, S.C. Srivastava and Ashwani Kumar

Abstract: **Available transfer capability (ATC) is a measure of the unutilized transfer capacity in the transmission network available for further commercial transaction over and above already committed uses. The present paper proposes the application of bifurcation criteria for ATC determination. Hopf bifurcation limit has been considered for determination of the dynamic ATC and saddle node bifurcation limit and bus voltage limit for the static ATC. The proposed method is applied for various bilateral transactions on 9-bus WSCC and 39-bus New England systems. Available transfer capability can be enhanced using FACTS controllers. In the present work, the use of SVC has been studied for the enhancement of the system ATC.**

Index Terms: **Dynamic available transfer capability, FACTS controllers, Hopf bifurcation, Saddle node bifurcation, Static var compensator.**

I. INTRODUCTION

The electrical utilities are getting restructured in several countries throughout the world, so as to introduce competition at generation and distribution levels while retaining the transmission network as a natural monopoly for techno-economic reasons. It is expected to overcome the inefficiency prevalent in the monopoly franchise structure with assured revenue collection. In a restructured environment, all generation companies (GENCOs) and distribution companies (DISCOs) try to bid for the most profitable transactions. It may therefore result in a very different generation and load dispatch schedule. Some part of the transmission system may get congested and overloaded as it is bound to provide fair access to all the market participants. For the sake of system security and reliability, it is required to assess the transmission system capabilities along different corridors beforehand.

In this context, NERC (North American Reliability Council)[1] has defined 'Available Transfer Capability (ATC) as a measure of power transfer capability remaining in the physical transmission network for further commercial activity over and above the already committed uses'. In other words, it is the additional amount of power that can be transferred over the network with margins for a range of uncertainties and contingencies when power is injected and extracted at the specified seller and buyer buses, respectively.

Sanjay K. Chaudhary is with the HVDC Division, Asea Brown Boveri (ABB) Ltd., New Delhi.
S.C.Srivastava is with the Department of Electrical Engineering, Indian Institute of Technology, Kanpur. e-mail: scs@iitk.ac.in
Ashwani Kumar is with the Electrical Engineering Department. at National Institute of Technology, Kurukshetra and presently pursuing his Ph.D at IIT-Kanpur. e-mail: ashwa@iitk.ac.in

Ejebe et al [2] used continuation power flow to find the load flow solution over the entire feasible range while increasing the system loading and generation as per the transaction considered. Linearity properties of the DC load flow algorithm along with network connecting matrices were utilized for the fast determination of ATC in ref. [3].

Wollenberg et al [4] proposed power transfer distribution factors (PTDFs) based on DC load flow for quick assessment of ATC. To overcome the errors resulting from DC load flow assumptions such as considering nominal voltage at all buses, loss-less system and neglecting charging capacitance of the lines, an AC sensitivity based method was suggested [5]. An optimization based method [6] was proposed for assessing ATC in case of simultaneous transfers.

Literature survey on ATC determination reveals that most of the work has considered only the static limits as the system constraints. The dynamics of the system, as a whole, when subjected to small and large disturbances, has to be studied and analyzed for stability. ATC calculated with the dynamic stability limits is referred as dynamic ATC. Tuglie et al [7] included the dynamic constraints for the assessment of ATC

Bifurcation analysis has been applied to voltage stability studies [8]. Hopf bifurcation has been associated with dynamic voltage instability while Saddle Node bifurcation has been related to the steady state (static) voltage stability limit. However, bifurcation approach has possibly not been applied to ATC calculation. Apart from considering the static limits, application of bifurcation analysis would be a novel idea in the assessment of dynamic ATC.

Increased reactive power transmission losses restrict the power transfer in the lines. Load compensation and additional reactive power support is expected to improve the total transfer capability of the system and, thus, enhance the ATC. FACTS controllers, such as TCSC, SVC, TCSC, UPFC etc., will provide reactive power compensation to the system, in improving the ATC of the system as well as the system stability due to their better controllability.

In the present paper both static and dynamic ATC have been computed using saddle node bifurcation (SNB) and Hopf bifurcation (HB) limits. To study the impact of FACTS controller on improvement of static and dynamic ATC values, SVC has been considered. The results have been computed for WSCC 3-generator 9-bus and New England 10-generator 39-bus systems.

II. MODELING OF POWER SYSTEM COMPONENTS

Generator: Swing equations describes the mechanical dynamics of the generator. There are several models describing the field decay dynamics of the generator. In the present paper two-axis dynamic model has been used [9].

The dynamic equations for *i*-th machine are given below :

$$\dot{d}_i = ?_i - ?_s \quad (1)$$

$$M_i ?_i = T_{Mi} - \left[E'_{qi} - X'_{di} I_{di}\right] I_{qi} - \left[E'_{di} - X'_{qi} I_{qi}\right] I_{di} - D_i\left(?_i - ?_s\right) \quad (2)$$

$$T'_{doi}\dot{E}'_{qi} = -E'_{qi} - \left(X_{di} - X'_{di}\right) I_{di} + E_{fdi} \quad (3)$$

$$T'_{qoi}\dot{E}'_{di} = -E'_{di} + \left(X_{qi} - X'_{qi}\right) I_{qi} \quad (4)$$

where,

δ = Machine rotor angle (in radians).

ω = Rotor speed (pu).

M = Machine moment of inertia.

T_m = Mechanical input torque.

E'_q & E'_d = q and d axis induced voltages behind transient reactances.

I_q & I_d = q and d axis stator currents.

X_q & X_d = q and d axis stator steady state reactances.

X'_q & X'_d = q and d axis stator transient reactances.

E_{fd}= Voltage induced due field excitation.

The stator variables E'_{di} , E'_{qi}, I_{di}, and I_{qi} are related to the network variables $V_i \angle\theta_i$ by the following complex algebraic equations :

$$V_i e^{j\left(p/2 - d_i + q_i\right)} + \left(R_{si} + jX'_{di}\right)\left(I_{di} + jI_{qi}\right) - \left[E'_{di} + \left(X'_{di} - X'_{qi}\right) I_{qi} + jE'_{qi}\right] = 0 \quad (5)$$

The power balance equation at the generator terminals is given as,

$$P_i + jQ_i = \left(V_i\right)\left(I_{di} - jI_{qi}\right) e^{j\left(p/2 - d_i + q_i\right)} - P_{Li}\left(V_i\right) - jQ_{Li}\left(V_i\right) \quad (6)$$

where,

$$P_i + jQ_i = \sum_{k=1}^{n} V_i V_k y_{ik} e^{j\left(q_i - q_k - a_{ik}\right)}$$

$$d_i = \text{Angle of } \left[V_i e^{j(q_i)} + \left(R_{si} + jX_{qi}\right)\bar{I}_{Gi}\right]$$

$$\bar{I}_{Gi} = \left(\frac{P_{Gi} - jQ_{Gi}}{V_i e^{-j(q_i)}}\right)$$

Excitation System: IEEE Type DC-1 excitation system [10] has been considered in this paper. It represents field controlled DC commutator exciters with continuously acting voltage regulators.

By choosing $T_B = T_C$, the Transient Gain Reduction (TGR) is neglected. Further the limiter action has been neglected in the present work. The dynamic equations for this model are:

$$T_{Ei}\frac{dE_{fdi}}{dt} = -\left(K_{Ei} + S_{Ei}\left(E_{fdi}\right)\right) E_{fdi} + V_{Ri} \quad (7)$$

$$T_{Ai}\frac{dV_{Ri}}{dt} = -V_{Ri} + K_{Ai} R_{fi} - \frac{K_{Ai} K_{Fi}}{T_{Fi}} E_{fdi} + K_{Ai}\left(V_{refi} - V_i\right) \quad (8)$$

$$T_{Fi}\frac{dR_{fi}}{dt} = -R_{fi} + \frac{K_{Fi}}{T_{Fi}} E_{fdi} \quad (9)$$

where,

$S_{Ei}\left(E_{fdi}\right) = A_{ex} e^{\left(B_{ex} E_{fdi}\right)}$ field saturation function.

V_{Ri} = Regulator amplfier output Voltage.

K_{Ai}, T_{Ai} = Regulator amplfier gain and time constatnt

K_{Ei}, T_{Ei} = Exciter gain and time constant

R_{fi} = Exciter rate feedback

V_{refi} = Reference voltage setting

V = Generator Terminal voltage.

Network equations: Load-flow equations decide the operating point in terms of bus voltage and phase angle ($V\angle\theta$) for specified generation schedule and load dispatch.

The steady-state load-flow equations can be written as:

$$0 = -P_i - jQ_i + \sum V_i V_k Y_{ik} \exp\left(j\left(q_i - q_k - a_{ik}\right)\right) \quad (10)$$

where,

$P_i + jQ_i$ = Real and reactive power injected in the network at bus i.

$Y_{ik}\angle a_{ik}$ = Network Admittance between busses i & k.

$V_i \angle q_i$ = Voltage and phase at bus i.

From eq. (6) the injected real and reactive power at the generator buses is given as,

$$P_i + jQ_i = V_i\left(I_{di} - jI_{qi}\right) e^{j\left(p/2 + q_i - d_i\right)} - P_{Li}\left(V_i\right) - jQ_{Li}\left(V_i\right) \quad (11a)$$

Similarly, at the load buses, for i = m + 1,..., n we have ,

$$P_i + jQ_i = -P_{Li}\left(V_i\right) - jQ_{Li}\left(V_i\right) \quad (11b)$$

Combining eqs.(11a) & (11b) with eq. (10), for generator buses, the loadflow equation becomes,

$$0 = V_i\left(I_{di} - jI_{qi}\right) e^{j\left(p/2 + q_i - d_i\right)} - P_{Li}\left(V_i\right) - jQ_{Li}\left(V_i\right) - \sum_{k=1}^{n} V_i V_j Y_{ik} e^{j\left(q_i - q_i - a_{ik}\right)} \quad (12a)$$

and for load busses, these are,

$$0 = -P_{Li}\left(V_i\right) - jQ_{Li}\left(V_i\right) - \sum_{k=1}^{n} V_i V_j Y_{ik} e^{j\left(q_i - q_i - a_{ik}\right)} \quad (12b)$$

Dynamic Model of SVC: Fig.1 gives a block diagram representation of SVC, taken from refs [8]. The measurement module for sensing the voltage and converting it into dc feedback signal has been ignored as it has small time constant. Further, in this work, the upper and lower limits of the SVC have been ignored. The gain, K_R, is the reciprocal of the slope setting. K_R is usually between 20 per unit (5% slope) and 100 per unit (1% slope) on the SVC base. The regulator time constant, T_R is usually between 20 and 150 milliseconds.

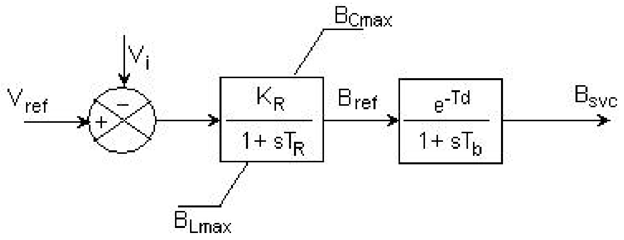

Fig 1 Dynamic Model of SVC

The time constant T_d is due to the time lag in the application of firing pulses corresponding to the new value of B_{svc}. T_b is the firing circuit time constant representing the effect of firing sequence and is typically of the order of 3 – 6 ms. The dynamic equations can be written as :

$$T_R \dot{B}_{ref} = -B_{ref} + K_R \left(V_{ref} - V_i\right) \qquad (13)$$

$$T_b \dot{B}_{svc} = -B_{svc} + B_{ref} \qquad (14)$$

At steady state,

$$B_{svc} = B_{ref} = K_R \left(V_{ref} - V_i\right)$$

and $Q_{svc} = V_i^2 \, B_{svc}$ (15)

Reactive power equations at a SVC bus 'm' can be written in a modified form as follows:

$$Q_m = V_m \sum_{k=1}^{n} Y_{mk} V_k \sin\left(q_m - q_k - a_{mk}\right) - V_m^2 \cdot B_{svc} \quad (16)$$

To include SVC in the load-flow model, the elements of the sub-matrix J_4 of Newton-Raphson load flow Jacobian, $[J] = \begin{bmatrix} J1 & J2 \\ J3 & J4 \end{bmatrix}$ can be modified as:

$$J4(m,m) = J4(m,m) - 2 \cdot V_m K_R \left(V_{ref} - \tfrac{3}{2} V_m\right) \quad (17)$$

where, $[J4] = \left.\frac{\partial Q_m}{\partial V_m} . V_m \right|_{(V,q)}$

III. ATC DETERMINATION USING BIFURCATION CONCEPT

According to NERC Report [9] ATC is defined as,

ATC = TTC – TRM – {ETC + CBM}

The existing transaction commitment (ETC) is known precisely only for the real time applications. For any other time interval in future, this has to be approximated by forecasting techniques. The ETC determines the base case operating point for the specified time interval. The transmission reserve margin (TRM) and capacity benefit margin (CBM) are decided as per the relevant policies of the system operator and the market participants. In general, the ATC without considering system margins is defined as:

ATC = TTC – ETC

Various operating margins such as Transmission Reserve Margin (TRM) and Capacity Benefit Margin (CBM) are to be accounted for separately when such definition is used for ATC determination. It shows the direct relationship between ATC and TTC. Hence all the constraints applicable to TTC are applicable to ATC and vice-versa.

The limits to be considered for the calculation of the transfer capability may be broadly classified as:

1.Static Constraints:
- Line Thermal Limits
- Bus Voltage (magnitude) Limits
- Saddle Node Bifurcation (Steady State Stability Limit)

2.Dynamic Constraints:
- Small Signal Stability Limit/Hopf Bifurcation Limit
- Large Signal Stability Limit.

The local stability of power systems can be evaluated by eigenvalue analysis of the system dynamic equations around the operating point. The system equations, both dynamic and algebraic, are linearized around a base operating point for this purpose

Bifurcation theory deals with the sudden change in the system behavior as certain system parameter called as bifurcation parameter (say p), is increased [11]. The change may be brought about by merging together of two distinct equilibrium points – one stable and the other unstable (Saddle Node Bifurcation) or by a pair of complex conjugate eigenvalues crossing the imaginary axis (Hopf Bifurcation).

Only the voltage limits and bifurcation limits are considered for ATC determination. The procedure used to include the bifurcation limits is given below:

A power system can be described by a set of dynamic and algebraic equations. The complex algebraic equations can be separated into real and imaginary parts. Symbolically these Differential Algebraic equations (DAE) can be denoted in brief as:

$$\dot{\mathbf{x}} = \mathbf{f}\left(\mathbf{x}, \mathbf{y}\right) \qquad (18)$$

$$\mathbf{0} = \mathbf{g}\left(\mathbf{x}, \mathbf{y}\right) \qquad (19)$$

Where,
x= Vector of dynamic state variables
y = Vector of algebraic variables

Eq (18) consists of Eqs. (1) to (4), Eqs. (7) and (9), while Eq. (19) consists of Eqs.(5) and (12) separated into real and imaginary parts. The algebraic variables, denoted by the vector **y**, depend upon the loading parameter, p. Solution of these equations at $\dot{\mathbf{x}} = \mathbf{0}$, then defines the initial operating point ($\mathbf{x_o}$, $\mathbf{y_o}$). The linearized equations for the incremental changes in variables over their initial values can be written as

$$\Delta\dot{\mathbf{x}} = \mathbf{A}\Delta\mathbf{x} + \mathbf{B}\Delta\mathbf{y} \qquad (20)$$

$$\mathbf{0} = \mathbf{C}\Delta\mathbf{x} + \mathbf{D}\Delta\mathbf{y} \qquad (21)$$

where,

$$\mathbf{A} = \left[\frac{\partial \mathbf{f}}{\partial \mathbf{x}}\right]_{\mathbf{x_o},\mathbf{y_o}}, \quad \mathbf{B} = \left[\frac{\partial \mathbf{f}}{\partial \mathbf{y}}\right]_{\mathbf{x_o},\mathbf{y_o}}$$

$$\mathbf{C} = \left[\frac{\partial \mathbf{g}}{\partial \mathbf{x}}\right]_{\mathbf{x_o},\mathbf{y_o}}, \quad \mathbf{D} = \left[\frac{\partial \mathbf{g}}{\partial \mathbf{y}}\right]_{\mathbf{x_o},\mathbf{y_o}}.$$

Solving for the value of vector, D**y**, from eq. (21) and substituting it in eq. (20) gives,

$$\therefore ?\,\dot{\mathbf{x}} = \left(\mathbf{A} - \mathbf{B}\mathbf{D}^{-1}\mathbf{C}\right)?\,\mathbf{x} \qquad (22)$$

where, $\tilde{\mathbf{A}} = \left(\mathbf{A} - \mathbf{B}\mathbf{D}^{-1}\mathbf{C}\right)$ is known as the reduced system Jacobian. The eigen-value analysis of reduced system Jacobian $\tilde{\mathbf{A}}$ has been used to find out the occurrence of Hopf bifurcation. Saddle node bifurcation has been identified by the non-convergence of Newton-Raphson load-flow algorithm.

IV. SIMULATION RESULTS

A WSCC 3-generator, 9-bus system and another New England 39-bus, 10-generator system have been taken as test systems for the present studies. Some typical transactions were considered between one of the load buses in the system and different generator buses. Saddle node bifurcation (SNB) and Hopf bifurcation (HB) limits have been used for determination of ATC. The ATC value corresponding to the HB gives the dynamic ATC, whereas that corresponding to the SNB provides the static ATC. In addition to these, the bus voltage limits have also been considered.

Voltage limits are considered at ±10% from the nominal value (1 pu). Apart from the values of TTC and ATC, the system real and reactive power losses and the buses experiencing low voltages in the system have also been analyzed in each case. The ATC and TTC have been computed in terms of only real power transactions expressed in p.u.

For ATC determination, the loading at the selected buses have been increased in the following two distinct ways:

1. Load1 – In this case, only the real part of the load is increased while the reactive part is assumed to remain constant. Such a case is referred in the following sections as ‘Load1’. This situation may arise in a deregulated market, if the consumer locally arranges for the reactive power requirement.

2. Load2 – In the second case, both real and reactive parts of the load has been increased in the same proportion such that the load power factor remains constant. This is referred as ‘Load2’ in the following sections. This case refers to a situation in deregulated market, when consumers also purchase the reactive power from the market.

In both the cases, the real power output of generators participating in the transaction has been increased by the amount of load change in the ratio of predefined generation distribution factors. The slack bus generator is assumed to supply the change in system loss. The results for the two systems are described below.

WSCC 3-generator, 9-bus System:

With the system load being increased at bus 5, the following transactions have been considered:

i) Transaction ‘T1’ Generator 1 alone supplies the increase in load at bus 5.
ii) Transaction ‘T2’ Generator 2 alone supplies the increase in load at bus 5.
iii) Transaction ‘T3’ Generator 3 alone supplies the increase in load at bus 5.
iv) Transaction ‘T4’ Generators at buses 1 and 2 equally share the increase in load at bus 5.
v) Transaction ‘T5’ Generators at buses 2 and 3 equally share the increase in load at bus 5.
vi) Transaction ‘T6’ Generators at buses 1 and 3 equally share the increase in load at bus 5.
vii) Transaction ‘T7’ Generators at buses 1, 2 and 3 are supplying the increased load in the ratio of 0.65, 0.25 and 0.10 respectively, chosen in approximate proportion to their respective machine inertia.

The ATC values obtained while considering the different limits viz. - voltage, Hopf bifurcation and saddle node bifurcation limits are depicted in Figs. 2&3. Due to excessive reactive power loading, the ATC values are much lower when voltage limits are considered than those in the previous cases corresponding to only bifurcation limits.

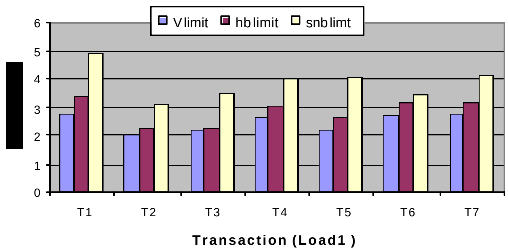

Fig. 2 ATC for WSCC 9-Bus System -Load1 Case.

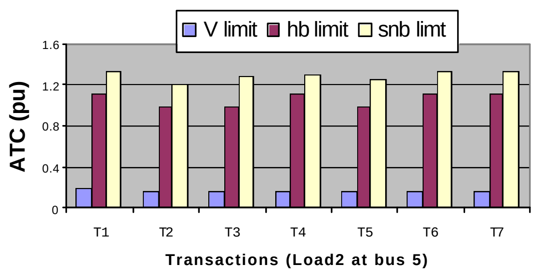

Fig.3 ATC for WSCC 9-Bus System -Load2 Case.

It is observed that the ATC values are lower in ‘Load2’ case as compared to ‘Load1’ case. Moreover, ‘Load2’ case results in poorer voltage profile.

39-bus, 10-Generator System: Following transactions were studied between load bus 18 and the specified seller (generator) buses:

i) Transaction 'T1' Generator 1 alone supplies the increase in load at bus 18.
ii) Transaction 'T2'Generator 2 alone supplies the increase in load at bus 18.
iii) Transaction 'T3'Generator 3 alone supplies the increase in load at bus 18.
iv) Transaction 'T4'Generator 8 alone supplies the increase in load at bus 18.
v) Transaction 'T5'Generator 10 alone supplies the increase in load at bus 18.

The charts given in Fig. 4 compares the ATCs obtained for different limits when only the real power demand at bus 18 is increased, while Fig. 5 compares the ATC for different limiting cases when both real and reactive power are increased.

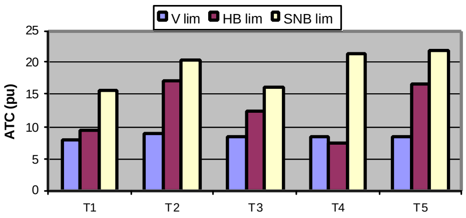

Fig. 4 ATC for 39 Bus System - Load1 Case

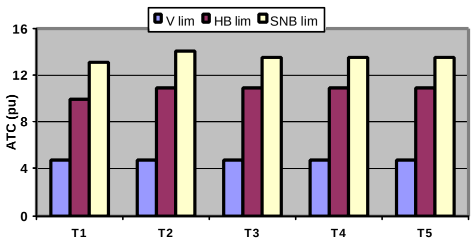

Fig. 5 ATC for 39 Bus System- Load2 Case

It is interesting to note that in almost all cases, the ATC is minimum when voltage limit is imposed except the 'Load1' and transaction T4 case in 39-bus system when the ATC with HB limit is the minimum.

V. SIMULATION RESULTS WITH SVC PLACEMENT

In the present paper, the state participation factor analysis [9] corresponding to the critical modes responsible for the Hopf Bifurcation (or saddle node bifurcation) has been used for optimal placement of SVC. SVC has been placed at a load bus having maximum voltage state participation factor corresponding to the critical mode.

For the different transactions and loading cases, the participation factors were calculated corresponding to the most critical eigenvalue. The load bus-5 for WSCC 9-bus system and load bus –18 for 39-bus New England system having the maximum voltage state participation factor corresponding to the critical mode were selected for the SVC placement.

In both the systems, a slope of 1% (the SVC output changes by 1 pu for 1% drop in voltage), which corresponds to the SVC regulator gain, K_R=100, has been considered. V_{ref} for SVC has been taken as 1 pu. T_R and T_b are taken as 50 ms and 6 ms, respectively [12].

WSCC 3-generator, 9-bus System: Figs.6 and 7 depict the ATC values of all transactions. While ATC values have increased after the placement of SVC for all the transactions, Hopf bifurcation is found to be the limiting constraint for ATC in most of the cases.

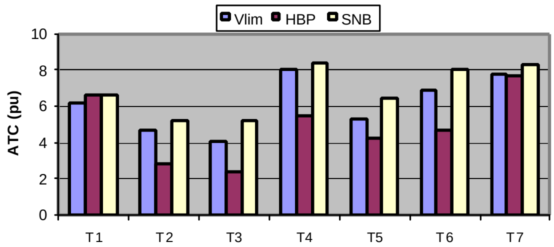

Fig. 6 ATC for 9 Bus System with SVC - Load1 Case

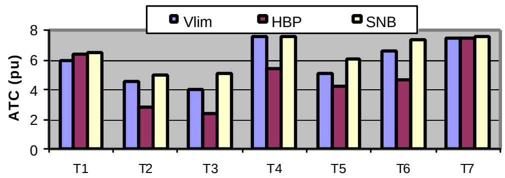

Fig. 7 ATC for 9-Bus System with SVC -Load2 Case

For all the transactions, except transaction – 'T1', the voltage profile at the lowest voltage busses are well above the minimum limit at the occurrence of Hopf Bifurcation. The corresponding ATC values are much higher than those for the cases without SVC, shown in Figs. 2 and 3.

For ATC with Saddle node bifurcation limit cases, though the bus-voltages drop below the minimum voltage limit of 0.9 pu at certain buses, the voltage profile is better than without SVC. The ATC values with SNB limits also increase when SVC is placed in the system.

The results for the simulations when both real and reactive power load at bus 5 are increased ('Load2') are shown Fig.5.Comparing the results with those shown in Fig. 7, it is found that ATC values and the voltage profile have improved in 'Load2' case also. The reactive power loss in the base case has slightly reduced with the introduction of SVC. While ATC values have increased after the placement of SVC for all the transactions, Hopf bifurcation is found to be the limiting constraint for ATC in most of the cases.

New England 10- generator 39-bus System: Figs. 8 and 9 compare the ATC for HB, SNB and bus voltage limit cases for 'Load1' and 'Load2' scenario, respectively. In most of the cases, Hopf bifurcation limits constrain the ATC value, whereas in quite a few cases voltage limits became the governing criteria.

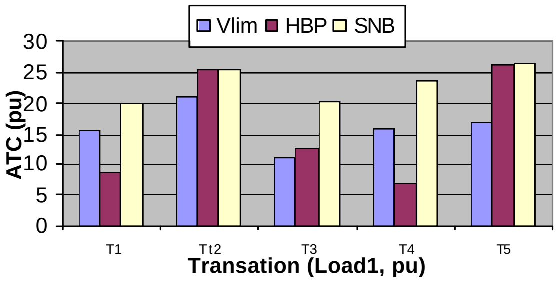

Fig. 8 ATC for 39-Bus System with SVC - Load1 Case.

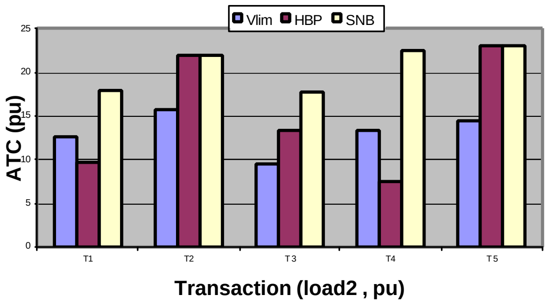

Fig.9 ATC for 39-Bus system with SVC -load 2 Case

In case of transactions T1 and T4, the bus voltages at HB are above the minimum bus voltage limits and hence HB becomes the corresponding limit for the ATC determination.

Figs. 8 and 9 presents the ATC values after placement of SVC at bus 18 for the two loading scenario. Comparing the ATC values shown in Figs.8 and 9 with the corresponding cases without SVC, it is observed that ATC values have increased in all the cases. Bus voltage profile has improved when SVC is considered in the system. In most of the cases, Hopf bifurcation limits constrained the ATC value, whereas in quite a few cases voltage limits became the governing criteria.

VI. CONCLUSIONS

1. For ATC determination, voltage limit criterion is found to be the limiting constraint in most of the transactions.
2. Hopf bifurcation occurs before saddle node bifurcation in most of the transactions studied. Hence, the dynamic ATC corresponding to Hopf bifurcation is found to be less than that corresponding to static ATC considering saddle node bifurcation. However, only in few cases Hopf bifurcation did not occur till the saddle node bifurcation.
3. Application of SVC at the load bus having maximum voltage state participation corresponding for the critical mode at the Hopf bifurcation and saddle node bifurcation is found to enhance the ATC value in all the cases. System voltage profile got improved after placement of the SVC.
4. With the placement of SVC, the Hopf bifurcation gets completely eliminated in few transaction cases e.g. transactions T2 and T5 in the 39-bus system 'Load2' case.
5. With the placement of SVC, Hopf Bifurcation criterion became the binding constraint for ATC in several transactions for both the systems e.g. transaction T1, T3 and T4 in 39-bus system 'Load1' case, T2 to T6 in the 9-bus WSCC system 'Load1' case.

VII. REFERENCES

[1] North American Electric Reliability Council (NERC), *Available Transfer Capability Definitions and Determination*, NERC Report, June 1996.

[2] G. C. Ejebe, J. Tong, G. G. Waight, J. G. Frame, X. Wang and W. F. Tinney, "Available Transfer Capability Calculations", *IEEE Trans. on Power Systems*, Vol. 13, No. 4, pp 1521-1527, Nov. 1998.

[3] G. C. Ejebe, J. G. Waight, M. Santos-Nieto and W. F. Tinney, "Fast Calculation of Linear Available Transfer Capability", *IEEE Trans on Power Systems*, Vol. 15, No. 3, Aug. 2000, pp. 1112-1116.

[4] R. D. Christie, B. F. Wollenberg and I. Wangensteen, "Transmission Management in the Deregulated Environment", *Proceedings of The IEEE*, Vol. 88, No. 2, Feb 2000, pp 170-195.

[5] R. Wang, R. H. Lasseter, J. Meng and F. L. Alvarado, "Fast Determination of Simultaneous Available Transfer Capability (ATC)", *PSERC Publications* 1999. Available at http://www.pserc.wisc.edu.

[6] G. Hamoud, "Assessment of Available Transfer Capability of Transmission Systems", *IEEE Trans on Power Systems*, Vol. 15, No. 1, Feb. 2000, pp. 27-32.

[7] E. D. Tuglie, M. Dicorato, M. L. Scala and P. Scarpellini, "A Static Optimization Approach to Assess Dynamic Available Transfer Capability", *IEEE Trans on Power Systems*, Vol. 15, No. 3, Aug. 2000, pp. 1069-1076.

[8] K. N. Srivastava, *Investigations Into Static and Dynamic Aspects of Voltage Stability*, PhD Thesis, IIT Kanpur, December 1994.

[9] P.Kundur, *Power System Stability and Control*, Mc. Graw Hill Inc., NY, 1994.

[10] K.R.Padiyar, *Power System Dynamics and Control*, John Wiley & Sons (Asia),Pte. Ltd., 1996.

[11] T. V. Cutsem and C. Vournas, *Voltage Stability of Electric Power Systems*, Kluwer Academic Publishers, USA, 1998.

[12] S.K. Chaudhary., Available Transfer Capability Assessment in a Restructured Electricity Market using Bifurcation Criteria, M.Tech Thesis, Department of Electrical Engineering, IIT Kanpur, January 2002